Optical trapping induced by reorientational nonlocal effects in nematic liquid crystals

L. Lucchetti,* L. Criante, F. Bracalente, F. Aieta, and F. Simoni
Dipartimento di Fisica e Ingegneria dei Materiali e del Territorio and CNISM, Università Politecnica delle Marche, via Brecce Bianche, I-60131 Ancona, Italy
(Received 5 May 2011; published 4 August 2011)

We report a detailed analysis of optical trapping of low index particles in liquid crystals under experimental conditions that prevent the effect of conventional trapping originated by optical gradient forces. The observation of stable, long-range trapping shows that this phenomenon in liquid crystals is regulated by a completely different mechanism than in isotropic media. In particular, the role of the nonlocality of optical reorientation is highlighted by showing the dependence of the trapping force on the size of the reoriented area. A model based on the actual form of the Gaussian focused beam impinging on the liquid-crystalline medium in the trapping experiment is also reported, with good agreement with experimental data.

DOI: 10.1103/PhysRevE.84.021702 PACS number(s): 42.70.Df, 87.80.Cc

I. INTRODUCTION

Recently there has been increased interest in optical trapping and manipulation of micrometric colloids dispersed in liquid crystals [1]. Because of the peculiar properties of the hosting medium, colloids with refractive indices lower than those of the liquid crystal can be efficiently trapped [2]. This effect is not possible in isotropic media in the case of single Gaussian beam trap. This is because optical trapping induced by gradient forces requires $m > 1$, where m is the ratio of the refractive index of the colloidal sphere to the one of the surronding medium. In the case of liquid crystals, it is also remarkable the range of the interaction (i.e., the distance from the focal spot where the trapping force is still active) is much bigger than the colloid size. Two different regimes have been considered for optical trapping of low-index particles, depending on the intensity of the trapping beam [3]. At light intensity lower than the threshold necessary to induce the optical reorientation in the hosting liquid crystal, trapping is ascribed to conventional gradient forces acting on the colloid, whose refractive index is modified from the liquid crystal distortion around it. In this way, it appears as a dressed colloid whose effective refractive index is higher than the one of the surrounding medium. Above the threshold for optical reorientation, trapping is due to the interaction between the colloid and the optically distorted region in the trap area. This trapping effect is a consequence of the elasticity and the long-range orientational order of the nematic liquid crystal. It is similar to what happens between two colloids in a liquid crystal: The orientational distortion induced by the inclusion of colloids increases the free energy of the medium, which consequently must reorient itself to minimize the energy. This occurs when the colloids are closely packed.

In a recent paper [4], we highlighted the strong relationship between optical trapping of low-refractive-index colloids and the light-induced optical reorientation in the trap area. In particular, we demonstrated that the trapping velocity is related to the optically induced phase shift due to the director reorientation produced in the liquid crystal by the laser beam creating the trap. Such a relationship confirms that the trapping mechanism in liquid crystals is different from the "ordinary" one and suggests that it is regulated by parameters not related to the traditional gradient force. Moreover, the need to claim two regimes for trapping is questionable because we expect a thresholdless optical reorientation when acting with a strongly focused beam on a liquid-crystalline cell. This has been observed recently by Brasselet [5,6] and is confirmed by our calculations in Sec. III.

In order to get away from the issue of two trapping regimes in the investigation of optical trapping of low-index particles in higher index nematics, we have chosen experimental conditions that prevent the onset of conventional gradient trapping. An objective with numerical aperture $NA = 0.45$ was used to create the optical trap. This value of NA is usually below the minimum value required to get stable optical trapping in isotropic media [7]. This point was actually checked by calculating the conventional trapping efficiency in the geometrical optics approximation (which describes our experimental conditions well), showing that conventional trapping is forbidden for all the values of the optical power.

The possibility of obtaining long-range stable trapping with this objective actually demonstrates that trapping in liquid crystals is totally different from optical trapping in isotropic media and is due to the elastic interaction between the optically distorted trap area and the colloid with its surrounding elastically distorted region, as pointed out by Skarabot *et al.* [3]. Our experimental results confirm their observation and point out additional features of the trapping phenomenon. Moreover, the long range of the interaction as compared to the size of the focal spot underlines the important role of nonlocality of the optical reorientation in this process.

The nonlinear optical distortion induced by the incident laser beam on the liquid crystal was measured by means of self-phase modulation during the trapping experiment, while tracking of the trapped particle movement was performed.

Director distortion was also analyzed by means of a model where the proper expression of the optical field of a focused beam and its propagation in a nematic liquid crystal were taken into account. Both the amount and the

*l.lucchetti@univpm.it

width of the induced director distortion have been derived by computer simulations based on the model. The results of the model have been successfully compared to the experimental data.

II. RESULTS ON OPTICAL TRAPPING

Optical trapping experiments were carried out on 50-μm-thick cells filled by a mixture of spherical silica particles with average radius $R_b = 2.5$ μm and refractive index $n_s = 1.37$, dispersed in the nematic liquid crystal pentyl-cyanobiphenil (5CB). The refractive indices of 5CB at $\lambda = 532$ nm are $n_o = 1.54$ and $n_e = 1.71$. The particles' surface was covered by N,N-dimethyl-noctadecyl-3-aminopropyl-trimethoxysilyl chloride (DMOAP) following the procedure described in [3], which gives rise to strong homeotropic anchoring at the particle surface. Cell substrates were also covered by DMOAP in order to obtain samples with homeotropic alignment. The refractive index of the particles is lower than both those of 5CB; nevertheless, optical trapping is possible, as described in previous publications [2–4].

We used a frequency-doubled Nd:YVO_4 laser (Coherent, Verdi V2) at $\lambda = 532$ nm as the light source in a classic inverted microscope configuration. The laser light was focused on the cell by a 20× microscope air objective with $NA = 0.45$. The optical power of the Gaussian linearly polarized beam impinging on the sample varied in the range 8–180 mW. In order to work in unfavorable conditions for conventional trapping, besides using a numerical aperture less than 0.7, trapping experiments were performed in underfilling conditions; that, is the laser beam waist is lower than the radius of the back aperture of the objective (see the discussion below).

Stable trapping of silica particles was observed for all the values of the used incident optical power. We selected an isolated particle approximately in the middle of the cell and positioned the trap in the same plane at different distances from the colloid, in the range of several tens of microns. Once the laser was switched on, the particle was attracted toward the focus and the movement was video recorded by means of a Carge-coupled device (CCD) camera at a rate of 25 frames/s. Different trajectories from several starting points around the trap center were observed, similar to what was reported in [3], clearly showing the anisotropic behavior of the trapping event. The particle changed its trajectory depending on the starting position and only for a particular direction (i.e., parallel to the beam initial polarization), and the movement followed a straight trajectory. Our experimental tracking results refer to this latter situation.

In order to check the role of conventional optical trapping in the stable trap observed in our geometry, we have evaluated the trapping efficiency under the geometrical optical approximation following the same approach described in [7]. The ray optics regime is well justified in our experiment since the dielectric particle is large compared to the wavelength ($2R_b \geqslant 10\lambda$).

We calculated the scattering, gradient, and total forces acting on the particle when both its center and the focus of the trapping beam are located along the z axes. We first found the scattering force dF_s and the gradient force dF_g due to a single ray entering the input aperture of the objective at an arbitrary radius $\tilde{r}$ from the beam axes and angle β from the vertical zy plane:

$$dF_s = \frac{n_m}{c}\left\{1 + R\cos 2\theta_i - \frac{T^2[\cos(2\theta_i - 2\theta_r) + R\cos 2\theta_i]}{1 + R^2 + 2R\cos 2\theta_r}\right\} dP = \Sigma(\tilde{r})dP, \tag{1a}$$

$$dF_g = \frac{n_m}{c}\left\{R\sin 2\theta_i - \frac{T^2[\sin(2\theta_i - 2\theta_r) + R\sin 2\theta_i]}{1 + R^2 + 2R\cos 2\theta_r}\right\} dP = \Gamma(\tilde{r})dP, \tag{1b}$$

where θ_i and θ_r are the incidence and refraction angles of the ray on the particle surface, R and T are the Fresnel reflection and transmission coefficients of the surface at angle θ_i, n_m is the average refractive index of the surrounding medium, and $dP = I(\tilde{r})\tilde{r}\,d\tilde{r}\,d\beta$ is the power of the single ray [see below for the definition of the input beam intensity $I(\tilde{r})$].

These formulas were integrated numerically over the distribution of input rays, taking into account that, by symmetry considerations, the total force is axial, so the contribution of each ray is given by $dF_{sz} = dF_s\cos\phi$ and $dF_{gz} = -dF_g\sin\phi$, when the center of the particle is located below the focus ($z > 0$). The angle ϕ, formed by the beam with the z axis, is connected to the incidence angle on the surface of the particle by the relation $R_b\sin\theta_i = S\sin\phi$, where S the distance between the particle center and the focus location. The integration was performed over the input aperture surface of the objective A_{AP} up to a maximum radius r_{max}, for which $\phi = \phi_{max} = 9^\circ$ is the maximum convergence angle for an objective with $NA = 0.45$ in 5CB with a filling factor $b = 0.5$:

$$F_S = \iint_{A_{AP}} dF_{SZ} = \int_0^{2\pi} d\beta \int_0^{r_{max}} \Sigma(\tilde{r})\cos\phi(\tilde{r})I(\tilde{r})\tilde{r}\,d\tilde{r}, \tag{2a}$$

$$F_G = \iint_{A_{AP}} dF_{gZ} = \int_0^{2\pi} d\beta \int_0^{r_{max}} \Gamma(\tilde{r})\sin\phi(\tilde{r})I(\tilde{r})\tilde{r}\,d\tilde{r}, \tag{2b}$$

considering the fundamental trasversal electro-magnetic mode intensity profile for the input beam (waist w_0 and power P) of the form

$$I(\tilde{r}) = \left(\frac{2P}{\pi w_0^2}\right)\exp\left(\frac{-2\tilde{r}^2}{w_0^2}\right). \tag{3}$$

The total force was obtained by adding the two contributions.

The filling factor b is defined as the ratio between the beam waist w_0 and the radius of the back aperture of the objective. The given value indicates that the incident beam does not completely fill the aperture, resulting in a trapping efficiency which is not optimized. The calculated forces as functions of the position along z are reported in Fig. 1(a) for our experimental conditions.

The value 1.11 for the ratio m between the refractive index of the colloid and the one of the surrounding medium was chosen in agreement with the hypothesis of the "dressed" particle proposed in [2,3]. We assigned the extraordinary

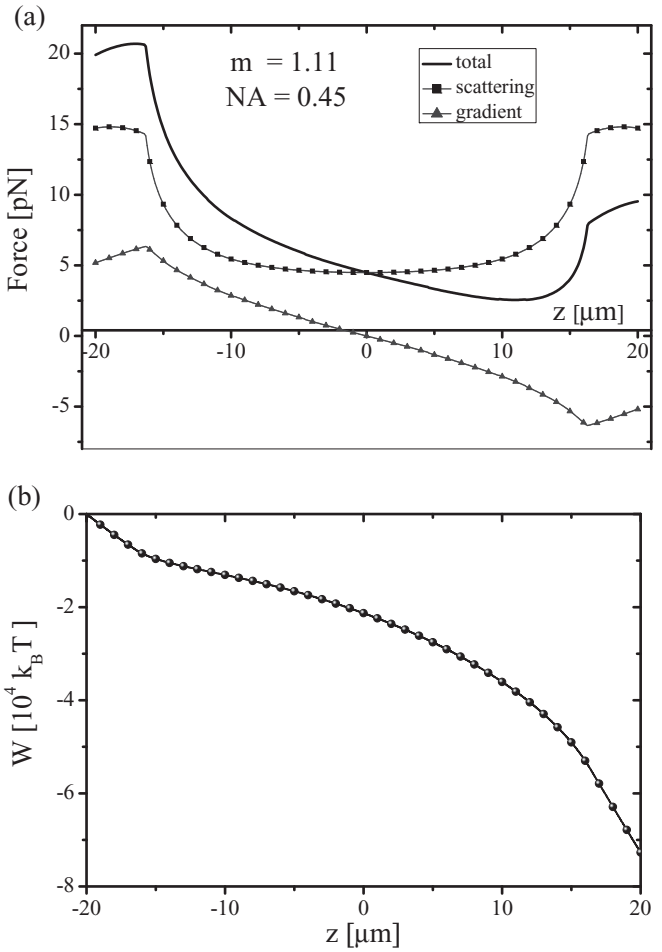

FIG. 1. (a) Scattering, gradient, and total forces acting on the particle during optical trapping vs distance acting between particle center and trap focus (origin along the z axis). The parameters used in the calculus are $m = 1.1$, $NA = 0.45$, and $P = 92$ mW. Positive (negative) forces correspond to repulsion (attraction). It is observed that the total optical force is positive for each value of z; that is, conventional trapping is not allowed. (b) Potential energy W vs particle position.

refractive index of 5CB to the distorted area around the colloid and the ordinary one to the region surrounding the dressed particle having homeotropic alignment. The former is the maximum index seen by the polarized laser beam corresponding to the colloid with homeotropic alignment on the surface, The total force is positive (repulsive) for every value of z, which means that no stable conventional trapping is allowed in our experimental conditions. This is also evident by looking at the shape of the potential energy profile W in Fig. 1(b), obtained by integration of the total force along the z axis. No well is observed.

By varying the values of m and NA in the calculation, we used the potential profile and the corresponding well depth (trap depth) to obtain the minimum trapping power required for longitudinal confinement of the particle. We defined the minimum trapping power as the power that provides a trap depth of $10k_BT$, a value generally accepted for particle confinement, in the weakest (backward) direction of the trap (i.e., below the focal point, $z > 0$ [8]).

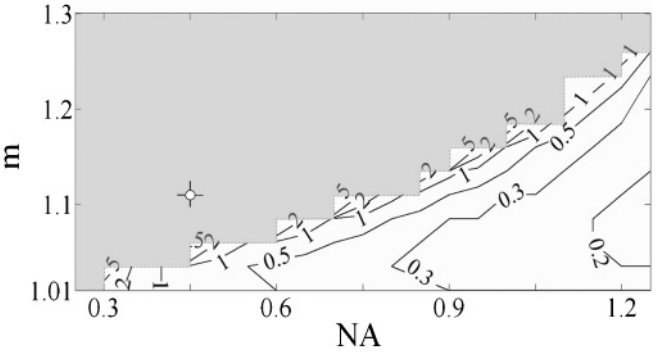

FIG. 2. Contour lines showing the minimum trapping power (mW) as function of m and NA. Dashed lines separate the trapping region from the no-trapping one, represented as a grey area. The check point indicates the working point in our experiment.

Figure 2 shows a contour plot of the calculated minimum trapping power as function of m and NA, for a filling factor $b = 0.5$. As mentioned, this value of b corresponds to underfilling the objective. The contour lines represent levels of constant powers in milliwatts, whereas the grey area is the region where conventional trapping is forbidden.

For the parameters leading to the results of Fig. 1, we get a point falling in the grey area.

This calculation points out that conventional trapping does not play any significant role in our case; therefore if a stable optical trap along the z axis is obtained, it cannot be connected to the conventional trapping conditions. Therefore, another mechanism is responsible for the effect.

The typical dependence of the particle displacement r vs time is reported in Fig. 3 for different values of the optical power. Here the latest value of r is the equilibrium distance (r_{eq}) from the center of the trap. This value of r varies with the optical power and is different from zero for every value of P.

The general trend is very similar to that usually reported for optical trapping in liquid crystals with conventional high

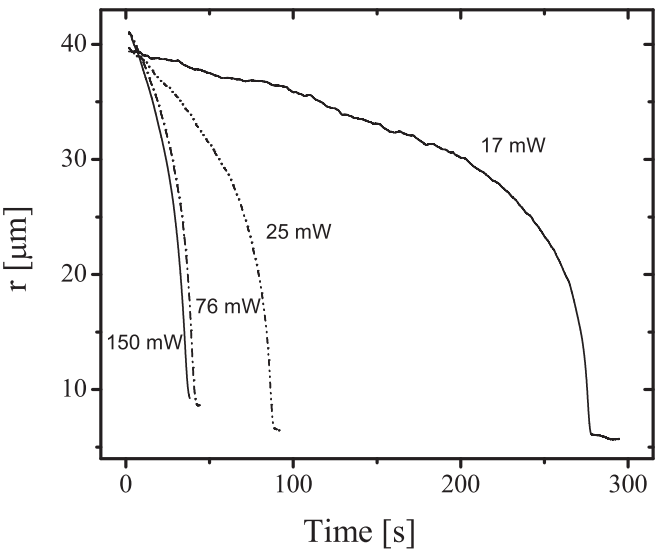

FIG. 3. Position of the particle vs time during trapping. The final value of r is the equilibrium particle distance r_{eq} from the center of the trap.

NA objectives [3,4]. An extensive analysis of several trapping experiments on different samples showed that the range of interaction between particle and laser beam can be as large as 45 μm.

Following the usual approach [3,9], the force between the laser focus and the silica particle was calculated assuming that it is nearly balanced by the drag force $F_D = 6\pi R\eta\frac{\partial r}{\partial t}$. In fact, the measured inertial force is much smaller than the viscous drag due to the small value of the particle mass ($M \approx 10^{-13}$ Kg), and thus in the motion equation it is always negligible. Moreover, the particle motion is highly viscously damped, allowing us to directly determine the attractive force from the displacement data by differentiating them to obtain the particle speed. For the viscosity, we used the expression $\eta = \frac{1}{2}\alpha_4$, where α_4 is one of the Leslie coefficients, holding when the flow is orthogonal to the director and producing a significant tilt of the molecular orientation [10]. For homeotropically aligned 5CB, we obtain $\eta = 0.028 Pas$.

Figure 4(a) shows the typical behavior of the trapping force vs particle-trap distance from the trap center (the negative sign is again chosen for attractive forces). The reported curve corresponds to the optical power $P = 92$ mW. The same behavior of $F(r)$ is obtained for all the optical power used in the experiment. The only difference is the equilibrium position that changes with power and is in this case $r_{eq} = 8.8$ μm (see discussion below).

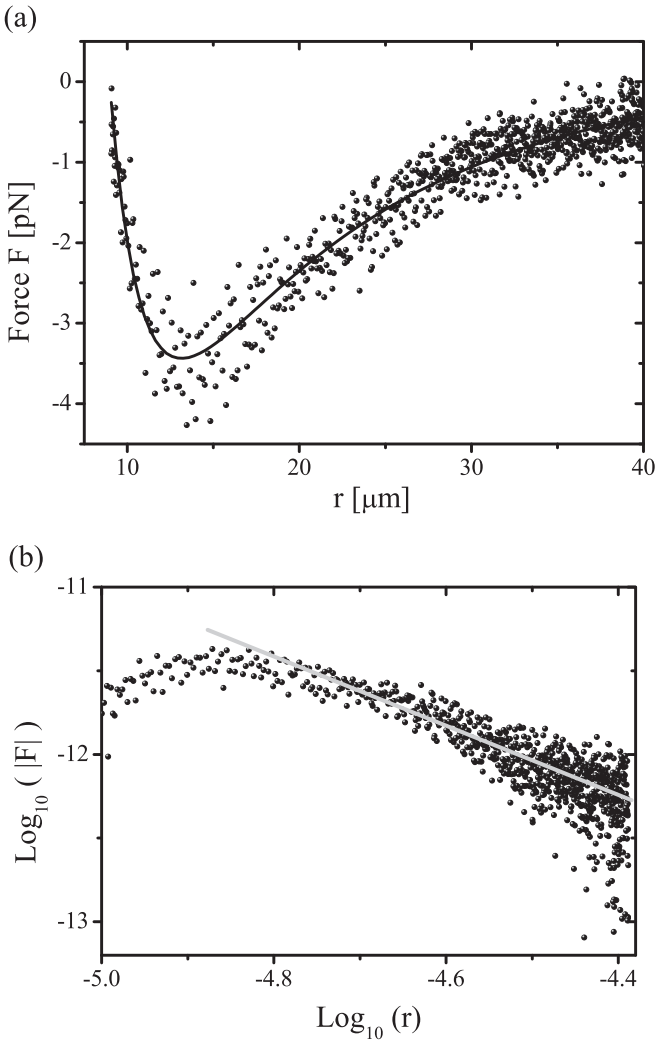

FIG. 4. (a) Typical shape of the trapping force acting on the silica particle vs the distance from the trap focus. The solid line is the best fit using Eq. (4); see text for details. (b) Logarithmic plot with the linear fit valid at long distance.

The attractive force increases as it approaches the trap until it reaches a maximum, decreases at a short distance with decreasing r, and eventually vanishes. The logarithmic plot shows a dependence on $r^{-\alpha}$ at long distance with $\alpha \approx 2$ [Fig. 4(b)]. From more than 50 measurements of trapping events, the average exponent α was obtained as -2.11 ± 0.08. At shorter distance, the dependence is different, and the overall curve is well described by the function

$$F = -\frac{A}{r^2} + \frac{B}{r^3}. \tag{4}$$

The solid line in Fig. 4(a) is the fit using this latter expression. A and B are constants whose value is given by the fitting procedure and is related to the strength of the two terms. The attractive Coulomb-like dependence is in agreement with what already reported for the same system [3,11].

As already pointed out [11], the interaction between a laser-induced reoriented nematic and a colloid cannot be considered as the interaction between two colloids even if conceptual similarities are possible. On the other hand, it is questionable to treat light-induced reorientation as a dipolar or quadrupolar symmetry defect, since symmetry, size, and amount of induced distortion are supposed to vary with optical power. However, by comparing the observed phenomenon to the interaction between two colloids or droplets in a liquid-crystalline host, it is quite interesting that in case of defects with dipolar symmetry an attractive term scaling with r^{-4} and a repulsive term scaling with r^{-6} have been obtained and experimentally demonstrated [12,13]; in our case, these terms scale as the square root of the ones of the former case, namely r^{-2} and r^{-3}.

Lev *et al.* [11] were able to justify the Coulomb-like attractive interaction in the case of a spherical particle of dipolar symmetry trapped by a light-induced reoriented area. Possibly similar arguments could justify the r^{-3} dependence of the repulsive term. Even if a complete theory of this interaction is not the aim of this work, some remarks can be done on the A and B coefficients.

By following arguments similar to the ones used to treat the interaction between colloids [9], we can write the attractive part of the force as

$$F_A = -\frac{A}{r^2} = -\frac{CKa^2(P)}{r^2}, \tag{5}$$

where a is the radius of the light-induced reoriented area that is dependent on the light power, K is the elastic constant of liquid crystal, and C is a dimensionless constant. From this, we expect $F_A(r)/a^2(P)$ to be independent on the size of the distorted area, that is, independent of the optical power.

Measurements of $a(P)$ have been performed by looking at the distorted area between crossed polarizers (see the next section). For each value of P, we have considered the curve of the force $F(r)$ for medium-long distance where the term $1/r^2$ is the dominant one. In this way, we were able to plot $F(r)/a^2(P)$ for different values of P, as reported in Fig. 5. Data fall on

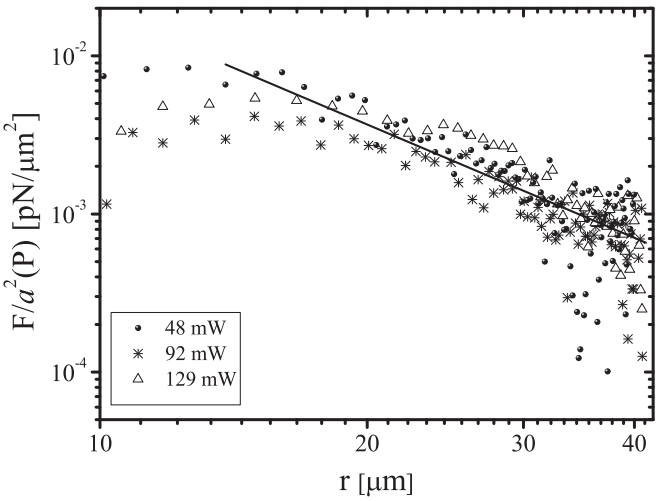

FIG. 5. Trapping force over the squared radius of the light-induced reoriented area vs the distance from the trap focus, for three different values of the power incident on the sample: $P = 48$ mW, $P = 92$ mW, and $P = 129$ mW. The log-log plot shows that data fall on a single curve. The solid line is the common linear fit.

a single curve, which confirms that the force scales as $a^2(P)$, pointing out that the dependence of the force on the optical power is due to the increasing width of the distorted area with increasing power.

Following a similar approach for the repulsive term, in agreement with the expression reported in [12] for colloid-colloid interaction, we may write

$$F_B = \frac{B}{r^3} = \frac{C' a^3(P)}{r^3}. \tag{6}$$

We have already pointed out that the particle equilibrium position changes by increasing power (as expected by the increase of the distorted area). According to our fitting curve

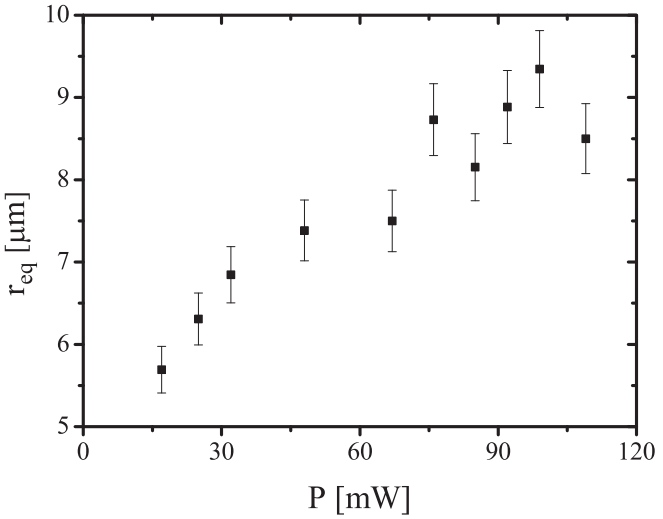

FIG. 6. Particle equilibrium distance from the trap focus vs trapping beam power.

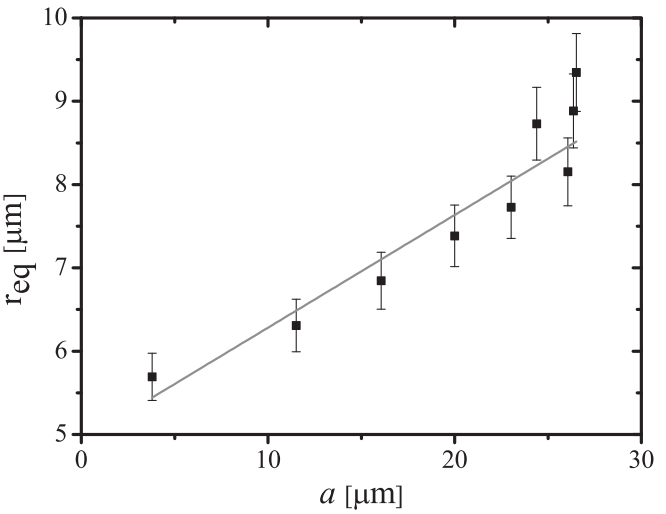

FIG. 7. Particle equilibrium distance from the trap focus vs the experimentally determined radius of the reoriented area. The solid line is the linear fit.

for the trapping force, the equilibrium position $F(r_{eq}) = 0$ is given by

$$r_{eq} = \frac{B}{A}, \tag{7}$$

that is, according to the expressions of F_A e F_B Eqs. (5) and (6),

$$r_{eq} = C'' a(P). \tag{8}$$

This means that we should expect a linear increase of the equilibrium distance vs the radius of the reoriented area. This is actually the case since the experimental values of r_{eq} vs P follow the linear dependence of a vs P before the occurrence of a saturation, as described in the next section.

In Fig. 6 the equilibrium distance r_{eq} from the center of the trap is reported as a function of the incident power P. For each power, the size $2a$ of the light-induced distortion was measured (see next section), and then we plotted the measured r_{eq} vs the measured $a(P)$ (see Fig. 7).

A clear linear dependence is evident in agreement with the above expression of B/A, confirming by independent measurements the consistency of this description for the trapping force. It is also interesting that at low incident power the equilibrium distance is $r_{eq} \cong 2.5\ R_b$ (where R_b is the particle radius), which is the same equilibrium distance observed between two colloids interacting in liquid crystals [13]. This might be a clue to the similarity between a real colloid and the light-induced distortion in the trap region at low optical power, before the size of this region becomes bigger than the one of the trapped colloid. However, further study is needed to address this point.

Finally, it is worth underlining that in our case a single trapping mechanism should work since the used fitting function is valid at all the used powers.

III. OPTICAL REORIENTATION UNDER STRONG FOCUSING CONDITIONS

We have shown in the previous section that while the focal waist of the laser beam is constant (about 0.6 μm in our

case) the effective area of director reorientation increases with power, reaching a radius close to 30 μm at the highest power used in the experiments. We have also shown the role of this strong nonlocality in the trapping mechanism. A further step in the analysis of this process can be done by evaluating the actual reorientation induced by the laser beam.

Light-induced reorientation in liquid crystals has been usually considered in the plane-wave approximation, which is generally fulfilled when the confocal beam parameter is much bigger than the sample thickness [14]. On the other hand, the effect of tighter focusing has been investigated by different authors [15–19], who have pointed out the strong nonlocality of the reorientation and the peculiar effects arising in the beam wave front. In all these previous works, the Gaussian distribution of the light intensity was taken into account, but the depolarization effect due to the wave-front curvature was neglected. In an optical tweezers apparatus, the strong focusing due to the objective makes such an approximation very weak. In fact, in this case the confocal beam parameter is much shorter than the sample thickness and actually several k vectors of the impinging wave are involved in the reorientation process together with the corresponding different polarizations. Recently Brasselet considered the effect of strong focusing of a circularly polarized beam on a liquid-crystalline film, pointing out the occurrence of no threshold reorientation and orientational defect in the center of the beam [5]. Here we describe the interaction of the optical field with the molecular director by using the field components calculated for a focused Gaussian beam. The aim is to evaluate the optical distortion induced in the medium in the region of the beam focus.

Let us consider a focused laser beam impinging on a homeotropic liquid-crystalline cell of thickness d, according to the geometry depicted in Fig. 8.

As usual, the free energy density of the system includes contributions due to the elastic and the optical torques [14]:

$$F_{\rm tot} = \frac{K_1}{2}(\vec{\nabla}\cdot\hat{n})^2 + \frac{K_2}{2}(\hat{n}\cdot\vec{\nabla}\cdot\hat{n})^2 + \frac{K_3}{2}(\hat{n}\times\vec{\nabla}\times\hat{n})^2 - \varepsilon_\perp\frac{|E|^2}{4} - \frac{\Delta\varepsilon}{4}(\hat{n}\cdot\vec{E})(\vec{n}\cdot\vec{E}^*), \quad (9)$$

where K_i are the elastic constants, **n** is the director, $\varepsilon_\perp$ is the ordinary dielectric constant, $\vec{E}$ is the optical field, and $\Delta\varepsilon$ is the dielectric anisotropy at optical frequencies.

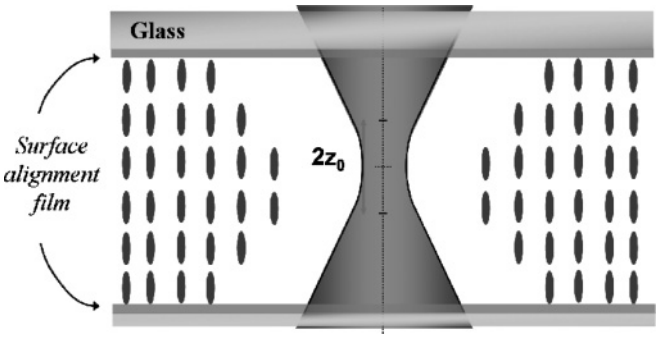

FIG. 8. Sketch of the geometry used in the model, corresponding to that used in the trapping experiments.

The total free energy of the system is obtained by integrating $F_{\rm tot}$ in the cell volume:

$$F = \int_0^\infty r dr \int_0^d dz \int_0^{2\pi} d\phi\,(F_{\rm tot}). \quad (10)$$

The induced liquid crystal reorientation can be obtained by minimizing the total free energy using the Euler-Lagrange equation. As mentioned, the optical field $\vec{E}$ to be used in the last term of Eq. (9) is the field associated with a focused beam. When a linearly x-polarized plane wave is focused by an aplanatic lens with numerical aperture $NA = n\sin\theta_{\max} = nR_L/f$ the field in the focal region in cylindrical coordinates reads [20]

$$E(\rho,\varphi,z) = \frac{ikf}{2}\sqrt{\frac{n_1}{n_{\rm eff}}}E_0 e^{-ikf}\begin{bmatrix} I_{00}+I_{02}\cos 2\varphi \\ I_{02}\sin 2\varphi \\ -2iI_{01}\cos\varphi \end{bmatrix}, \quad (11)$$

where k is wave-vector modulus, R_L is the aperture radius of the lens, f is the focal length, n_1 is the refractive index of the medium before the lens (air in our case), and $n_{\rm eff}$ is the effective refractive index of medium after the lens where the refracted beams travel.

The light focused by the objective travels in air, in glass, and in the liquid-crystalline medium before reaching the focal region. In order to assign a value to $n_{\rm eff}$ we performed an average over the optical paths in the three different media, obtaining $n_{\rm eff} = 1.23$.

It is clear from Eq. (11) that the optical field is depolarized and has nonvanishing components along the three spatial directions. The functions I_{00}, I_{01}, and I_{02} are defined as follows:

$$I_{00} = \int_0^{\theta_{\max}} f_w(\theta)\sqrt{\cos\theta}\sin\theta(1+\cos\theta)J_0 \times (k\rho\sin\theta)e^{(ikz\cos\theta)}d\theta,$$

$$I_{01} = \int_0^{\theta_{\max}} f_w(\theta)\sqrt{\cos\theta}\sin^2\theta J_1(k\rho\sin\theta)e^{(ikz\cos\theta)}d\theta, \quad (12)$$

$$I_{02} = \int_0^{\theta_{\max}} f_w(\theta)\sqrt{\cos\theta}\sin\theta(1-\cos\theta)J_2 \times (k\rho\sin\theta)e^{(ikz\cos\theta)}d\theta,$$

where J_n is the nth-order Bessel function and $f_w(\theta) = \exp(-f^2\sin^2\theta/w_0^2)$.

Now we can include Eq. (11) into Eq. (9), and we perform minimization of the total free energy by applying the Euler-Lagrange equation in the one elastic constant approximation. In this way, we get the following differential equation for the tilt angle θ:

$$K(\theta_r + r\theta_{rr} + r\theta_{zz}) + \frac{\Delta\varepsilon}{16}k^2f^2\frac{n_1}{n_{\rm eff}}rE_0^2[(D-H)\sin 2\theta + 2F\cos^2\theta] = \frac{\Delta\varepsilon}{16}k^2f^2\frac{n_1}{n_{\rm eff}}rE_0^2F. \quad (13)$$

Here K is the average elastic constant of the liquid crystal, θ_r and θ_z are the derivatives of θ with respect to r and z, and D, H, and F are constant parameters coming from the integral

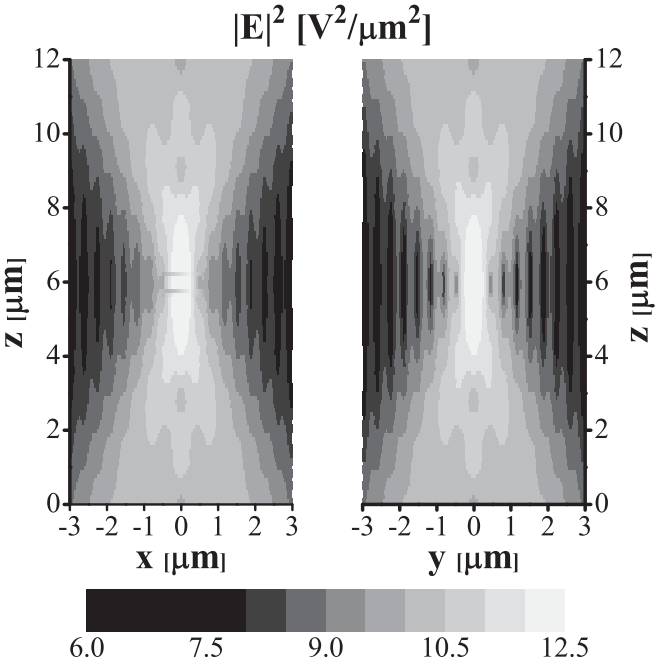

FIG. 9. Square modulus of the focused field E on the xz and yz longitudinal plane calculated from Eq. (11) for $NA = 0.45$. The shape of the fields justifies the radial symmetry approximation.

functions (12) to be numerically evaluated for each value of r and z. Their expressions are

$$D = |I_{00}|^2 + |I_{02}|^2 + (I_{00}I_{02}^* + I_{02}I_{00}^*),$$
$$H = 4|I_{01}|^2, \qquad (14)$$
$$F = 2i(I_{02}I_{01}^* - I_{02}^*I_{01} + I_{00}I_{01}^* - I_{00}^*I_{01}).$$

Before going on, it is worth noting that the integration over the azimuthal angle is fair as long as the radial symmetry is conserved. On the other hand, it is known that with increasing field confinement at the focus the focal spot becomes more and more elongated in the direction of polarization [20]; that is, the radial symmetry gets lost. However, if the objective NA is not too high, the departure from radial symmetry is small and the approximation can be maintained. This is shown in Fig. 9, where a computer simulation of the square modulus of the focused field $\vec{E}$ on the xz and yz planes, calculated from Eq. (11), are reported in the case of $NA = 0.45$, which is the value used in the experiments. The xz longitudinal section of the field appears only slightly broader with the respect to the yz longitudinal section, and thus the choice of radial symmetry is reasonable in this case.

Equation (13) has to be solved numerically. The finite difference method was used to calculate the tilt angle $\theta(r,z)$ as a function of the power incident on the liquid crystal. Computer simulations were carried on by using the same values for the parameters as those used in the experiment.

In Fig. 10, the tilt angle $\theta(r,z)$ is reported in a three-dimensional plot for an optical power $P = 30$ mW, in our experimental conditions. First of all, we should notice the peculiar behavior around the focal spot: The tilt angle changes

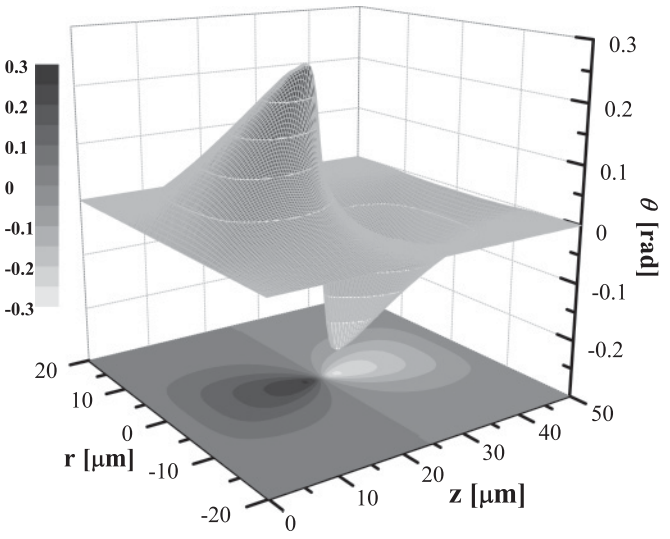

FIG. 10. Three-dimensional plot of the liquid-crystalline director distortion $\theta(r,z)$ induced by a focused Gaussian beam in case of $NA = 0.45$ and $P = 30$ mW. The vertical scale on the right represents values of the reorientation angle in radians.

the sign crossing z_f, that is, the location of the minimum cross section of the beam.

However, the important feature we analyze here is the nonlocality of the optical reorientation. In Fig. 11, the experimentally evaluated distorted area diameter is reported together with the values calculated from $\theta(r,z_f)$ at each optical power. We get a very satisfactory numerical model (dotted line) considering that the theoretical width between points was $\theta(r,z_f) > 0.1$ rad, which is the limit of detection of the microscopic observation of director reorientation.

The large values of the range of the reoriented region extension reported in Fig. 11 show that, despite the micron size of the beam waist, the incident light induces a much larger optical director distortion, up to 65 μm and more for power

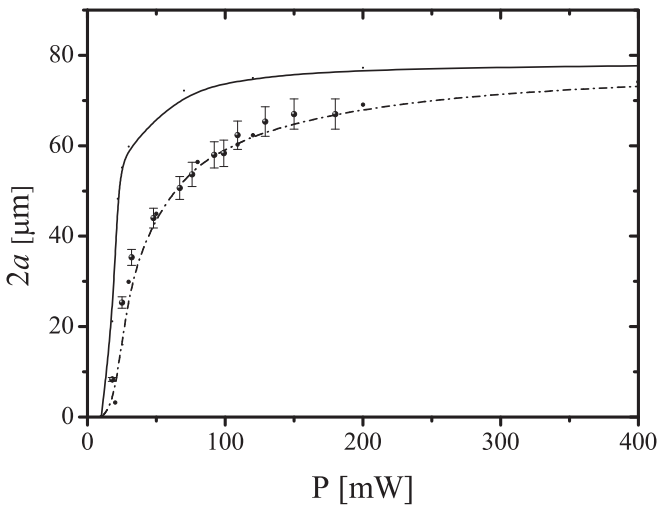

FIG. 11. Experimental values of the diameter of the distorted area (dots); simulated curve for a focused beam by an objective with $NA = 0.45$ (dashed line) and simulated curve for a weakly focused Gaussian beam (solid line).

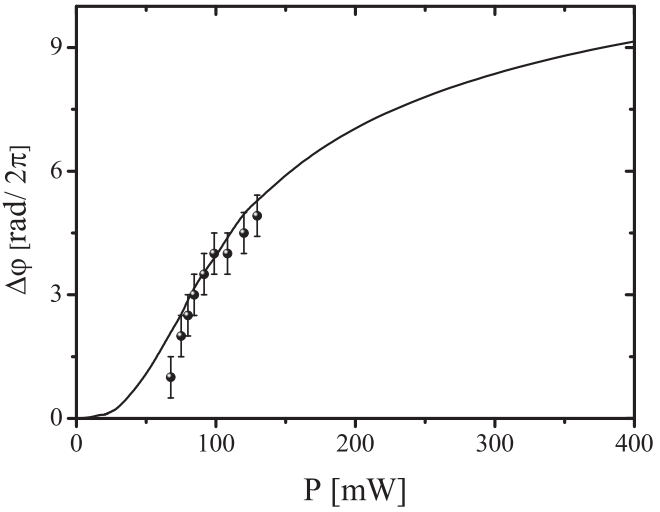

FIG. 12. Experimental (dotted line) and calculated (solid line) values of the light-induced phase shift vs the trapping beam power.

higher than 200 mW. We have shown how such nonlocality affects the trapping force (through A and B parameters) responsible for the long-range interaction between trap and colloid.

Performing the same calculation without taking into account the depolarization effect in the focal waist, we get the solid line, which is not able to fit the experimental data. It is quite interesting to see from this figure that the depolarization effect leads to a slower rise with power of the reoriented area.

From the calculated $\theta(r,z)$ we can also obtain the optically induced phase shift as $\Delta\varphi = \frac{2\pi}{\lambda}\int \delta n(r=0,z)dz$, where $\delta n = n(\theta) - n_o$. This quantity is shown in Fig. 12 as a solid line where it is compared to the same quantity evaluated by self-phase-modulation (SPM) experiments.

SPM measurements [14] allow monitoring of the nonlinear optical reorientation induced by the trapping beam in the trap area. They have been performed by recording the typical SPM ring pattern originated in the transmitted beam after focusing. Typical ring patterns are shown in Fig. 13 for different values of the incident power.

The maximum induced phase shift can be easily evaluated by the number of rings, through the relation $\Delta\varphi = 2\pi N$ [14].

It is worth emphasizing the absence of the thershold for optical reorientation shown in the theoretical curve. This behavior is not surprising, since when a focused beam is used a wide spectrum of incident wave vectors should be considered and a nonthreshold behavior can be expected for nonlinear optical reorientation. In fact no threshold effect occurs when an extraordinary wave is present, even at low incident power, as happens due to the depolarization effect of a strongly focused beam. Of course, this effect cannot be detected by simple SPM measurements able to monitor a minimum phase shift of 2π and a more sophisticated pump probe technique would be necessary to investigate the low-power reorientation leading to phase shift $\Delta\varphi < 2\pi$. We should mention that the evaluation of the induced phase shift during optical trapping through the pump-probe tecnhique was recently proposed [4,21]. Although trapping was performed with a higher NA objective ($NA = 1.2$) [4], samples were similar to those used here and a nonvanishing phase shift was measured also for low values of the incident intensity.

Also in this case the comparison of the experimental results with data obtained by computer simulation is very satisfactory, which means that the model is suitable to represent the interaction of a focused beam with the liquid-crystalline medium.

The value used here for the numerical aperture of the objective is the experimental value $NA = 0.45$. However, the model is of general validity, and the numerical aperture can be increased in order to consider the interaction when a high NA objective is used, typical of conventional optical trapping. A more detailed presentation of the model and its application to several different situations will be reported elsewhere.

An additional view of the dependence of the trapping force on the optical reorientation of liquid crystals can be given by

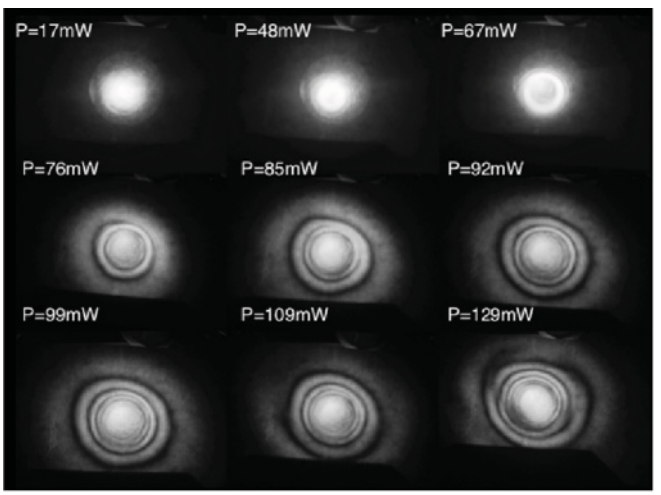

FIG. 13. SPM ring pattern for different values of the trapping beam power.

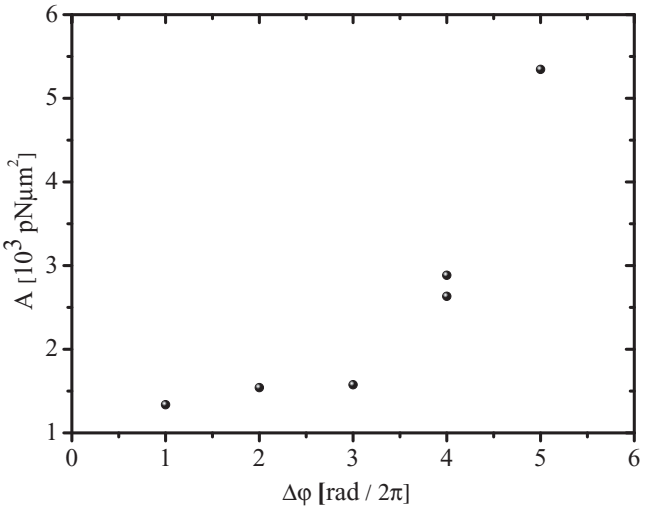

FIG. 14. Coefficient A [first term of Eq. (4)] vs the experimental light-induced phase shift.

the dependence of the parameter A affecting the r^{-2} term of the trapping force on the measured nonlinear phase shift, shown in Fig. 14. The increase of A with increasing $\Delta\varphi$ points out the strong relation between the observed trapping phenomenon and the light-induced director reorientation.

IV. CONCLUSIONS

We have investigated optical trapping of silica particles that have a refractive index lower than the ones of the surrounding nematic liquid crystal under experimental conditions ($NA = 0.45$ and $b = 0.5$) that prevent the effect of conventional trapping originated by optical gradient forces. The observation of stable, long-range trapping shows that this phenomenon in liquid crystals is regulated by completely different mechanism with respect to those working in isotropic media. The trapping force is of longer range (several tenths of micron) than the conventional one, and it includes an attractive term scaling as r^{-2} (already discussed in [9]) and a repulsive term scaling as r^{-3}. This behavior shows a stronger interaction than the one observed in the case of colloids or droplets with associated dipolar defects (scaling respectively with r^{-4} and r^{-6}). However, this comparison suggests an analysis of the power dependence of the parameters driving the attractive and the repulsive terms that demonstrates that the size a of the optically reoriented area affects the trapping force. Experimental data show a^2 dependence for the attractive term and a^3 dependence for the repulsive term. In other words, the strength of the interaction is regulated by the nonlocality of optical reorientation, since the width of the reoriented area a is more than one order of magnitude bigger than the focal waist.

In order to evaluate this parameter, we have also developed a model for light-induced reorientation in nematics by taking into account the depolarization effect of a strongly focused Gaussian beam. In this way, we could get good agreement with experimental data for both the width of optically distorted area and the nonlinear phase shift that can be measured on the laser trapping beam.

[1] For a review of the subject, see R. P. Trivedi, D. Engstrom, and I. I. Smalyukh, J. Opt. **13**, 044001 (2011).

[2] I. Musevic, M. Skarabot, D. Babic, N. Osterman, I. Poberaj, V. Nazarenko, and A. Nych, Phys. Rev. Lett. **93**, 187801 (2004).

[3] M. Skarabot, M. Ravnik, D. Babic, N. Osterman, I. Poberaj, S. Zumer, and I. Musevic, Phys. Rev. E **73**, 021705 (2006).

[4] F. Simoni, L. Lucchetti, L. Criante, F. Bracalente, and F. Aieta, Proceedings of the SPIE **7775**, 77750F-1 (Iam Choo Khoo, San Diego, 2010).

[5] E. Brasselet, J. Opt. **12**, 124005 (2010).

[6] E. Brasselet, Opt. Lett. **34**, 3229 (2009).

[7] A. Ashkin, Biophys. J. **61**, 569 (1992).

[8] P. Zemanek, A. Jonas, P. Jakl, J. Jezek, M. Sery, and M. Liska, Opt. Commun. **220**, 401 (2003).

[9] P. Paulin, D. Cabuil, and A. Weitz, Phys. Rev. Lett. **79**, 4862 (1997).

[10] P. G. DeGennes, *The Physics of Liquid Crystals* (Clarendon Press, Oxford, 1975).

[11] B. Lev, A. Nych, U. Ognysta, S. B. Chernyshuk, V. Nazarenko, M. Skarabot, I. Poberaj, D. Babic, N. Osterman, and I. Musevic, Eur. Phys. J. E **20**, 215 (2006).

[12] T. C. Lubensky, D. Pettey, N. Currier, and H. Stark, Phys. Rev. E **57**, 610 (1998).

[13] K. Takahashi, M. Ichikawa, and Y. Kimura, Phys. Rev. E **77**, 020703(R) (2008).

[14] F. Simoni, *Nonlinear Optical Properties of Liquid Crystals and Polymer Dispersed Liquid Crystals* (World Scientific, Singapore, 1997).

[15] F. Bloisi, L. Vicari, F. Simoni, G. Cipparrone, and C. Umeton, J. Opt. Soc. Am. B **5**, 2462 (1988).

[16] L. Csillag, I. Janossy, V. F. Kitaeva, N. Kroo, and N. N. Sobolev, Mol. Cryst. Liq. Cryst. **84**, 125 (1982).

[17] I. C. Khoo, T. H. Liu, and P. Y. Yan, J. Opt. Soc. Am. B **4**, 115 (1987).

[18] E. Santamato and Y. R. Shen, Opt. Lett. **9**, 564 (1984).

[19] L. Lucchetti, S. Suchand, and F. Simoni, J. Opt. A **11**, 034002 (2009).

[20] L. Novotny and B. Hecht, *Principles of Nano-optics* (Cambridge University Press, Cambridge, 2006).

[21] E. Brasselet, Phys. Rev. A **82**, 063836 (2010).